Analysis and Characterization of the Microstructure Properties for U–Zr Series Alloys

Zhiyong Bai, Jiancheng Liu and Xuewei Zhang

Abstract The microstructure of alloy has an important influence on the application as fuel elements in the reactor. By spray casting the U–2, 4, 6, 8 and 10 wt% Zr series alloy are prepared. Alloy samples are treated through homogenization annealing. In the paper, the transformation law of microstructure and performance of the alloy under different conditions was studied and the thermal physical properties of U–Zr series alloy were also obtained. The results show it will provide technical basis for the application of the U–Zr alloy fuel.

Keywords Microstructure · Homogenization annealing · Thermal physical properties · U–Zr series alloy

Introduction

Zirconium has a relative low cross section of thermal neutron. Thus uranium alloys with Zr have excellent corrosion resistance and dimensional stability in the thermal cycling. These advantages make the U–Zr alloy becoming excellent choice of fuel in nuclear reactor. As early as 1985, three kinds of fuel U–10Zr, U–8Pu–10Zr, U–19Pu–10Zr were tested in the EBR-II in the United States. Results show that the addition of Zr increases the compatibility between the alloy fuel and cladding material [1]. And the irradiation stability of U–Zr alloy fuel is closely related to the composition, phase structure and microstructure uniformity.

Z. Bai (✉) · J. Liu · X. Zhang
China North Nuclear Fuel Co. Ltd., 456, Baotou 014035, Inner Mongolia, China
e-mail: bzyzlqnm@163.com

J. Liu
e-mail: 690226911@qq.com

X. Zhang
e-mail: 969647786@qq.com

Y. Han (ed.), *Advances in Energy and Environmental Materials*,
Springer Proceedings in Energy, https://doi.org/10.1007/978-981-13-0158-2_8

The phase composition of U–Zr alloy and the phase transformation law during the heat treatment greatly affect the application of alloy fuel in the reactor operation. So far, U–Zr alloy are used as reactor fuel in as-cast form commonly. The research about U–Zr alloy casting and subsequent processing has been rarely reported. Thus, the microstructures of a series of uranium zirconium alloy with different states were studied to provide theoretical basis for further development and application of U–Zr alloy fuel in this paper.

Experiments

Firstly a series of U–Zr alloy samples with the Zr content of 2, 4, 6, 8 and 10 wt% were prepared by spray casting. Homogenization heat treatment was carried out on the samples. Metallographic microscope, XRD, scanning electron microscopy (SEM), energy dispersive spectrometer (EDS) were used to detect and analyze the alloy. The microstructure of as-cast alloy and alloy with different heat treatment were studied. At the same time alloy density, heat capacity (specific heat), thermal conductivity, thermal expansion coefficient and other physical performance of the U–Zr series alloy have been inspected.

Metallographic Tests. The polished and corrosion state of U–Zr alloy with different heat treatments were analyzed by metallographic microscope. The universal research level automatic metallographic microscope was used in the research with the models AxioObserverZ1m. At the same time the alloy composition is analyzed by Scanning Electron Microscopy (SEM) spectrometer (Model VEGA3XMU).

Phase Structure Analysis. The phase structure of U–Zr alloy was analyzed by X-ray diffract meter (model D8 Da Vinci). The scanning mode is 2θ with scan range from 10° to 90°. The step interval is 0.02°. And each step acquisition time is 0.02 s. The source is standard Cu Kα with a wave length of 0.154 nm. The work voltage of the X ray tube is 40 kV and the current is 40 mA.

Physical Performance Tests. The tests sample size is Φ20 mm. The thermal conductivity tests are conducted on thermal conductivity detection instrument (LSA457). The STA449F3 synchronous heat analyzer was used to measure the specific heat. And the thermal expansion coefficient was tested by the DIL402CD thermal expansion coefficient meter.

Results and Discussion

Microstructure Analysis of the Spray as-cast Alloy Sample. As-cast alloy sample polished is observed by the metallographic microscope. Figure 1 shows the polished states of U–2 wt% Zr and U–8 wt% Zr alloy. The surface of the specimen

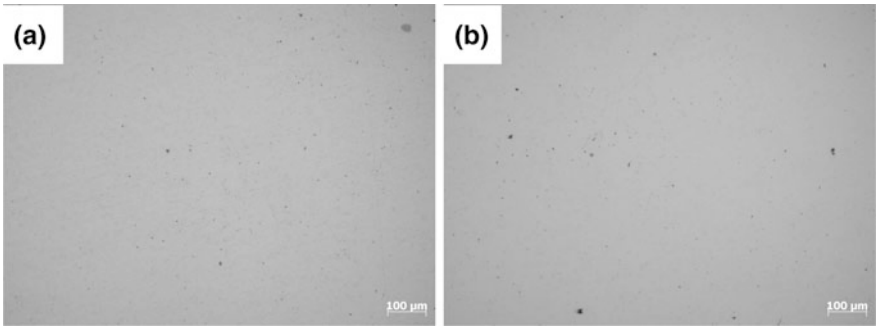

Fig. 1 Metallographic pictures of polished state for spray casting samples. **a** U–2 wt% Zr, **b** U–8 wt% Zr

is smooth. There are no obvious inclusion and incomplete fusion. The microstructure appearance of the other series alloy is similar as Fig. 1, which shows that the alloy prepared through the present melting process can be alloyed fully.

The corrosive states of the as-cast sample are shown in Fig. 2. Figure 2a is U–2 wt% Zr alloy. In the grey matrix there uniformly distributes small light phase. Figure 2b is U–4 wt% Zr alloys, the area light phase become bigger, with a fish-bone shape. And there is evident grain boundary. At the same time there appears some acicular structure within the grain boundary, which is similar to the acicular martensite. The states of U–6 wt% Zr and U–8 wt% Zr alloy are shown in Fig. 2c, d. The acicular structure is more visible in microscopic tissue. But it turns to be smaller. The microstructure of U–10 wt% Zr alloy appeared to be lath-like interleaved distribution. And the two phases show to be an alternative distribution. There are more and larger light color phase particles in U–10 wt% Zr alloy.

A spectral analysis of light phase of different alloys is shown in Fig. 3. The results show that it is U–56 wt% Zr. According to the phase diagram, during the cold process of melt, the Zr-rich phase will precipitate firstly, and then the structure of equilibrium is formed. The light colored parts of the alloy are considered to be Zr-rich phase, and the grey matrix is the α-U + δ phase (Fig. 4).

The acicular structure in the metallographic photograph is similar to that of the quenched α' phase in the U-rich alloy. In order to study the formation mechanism of acicular structure, the U–4 wt% Zr alloy sample was selected for quenching (metallographic pictures are shown in Fig. 5). And the acicular microstructure in the U–4 wt% Zr alloy after quenching is martensite. This is consistent with the microstructure of the as cast U–4 wt% Zr alloy sample. It shows that the cooling rate of melting in the mould is high in the spray molding process, which reaches the level of the quenching. In addition, with the further increase of Zr, acicular structure become small step by step until the microstructure of U–10 wt% Zr alloy reaching the lath-like interleaved distribution. It suggests that under the same process condition, the alloy phase transition resistance increases gradually and the metastable

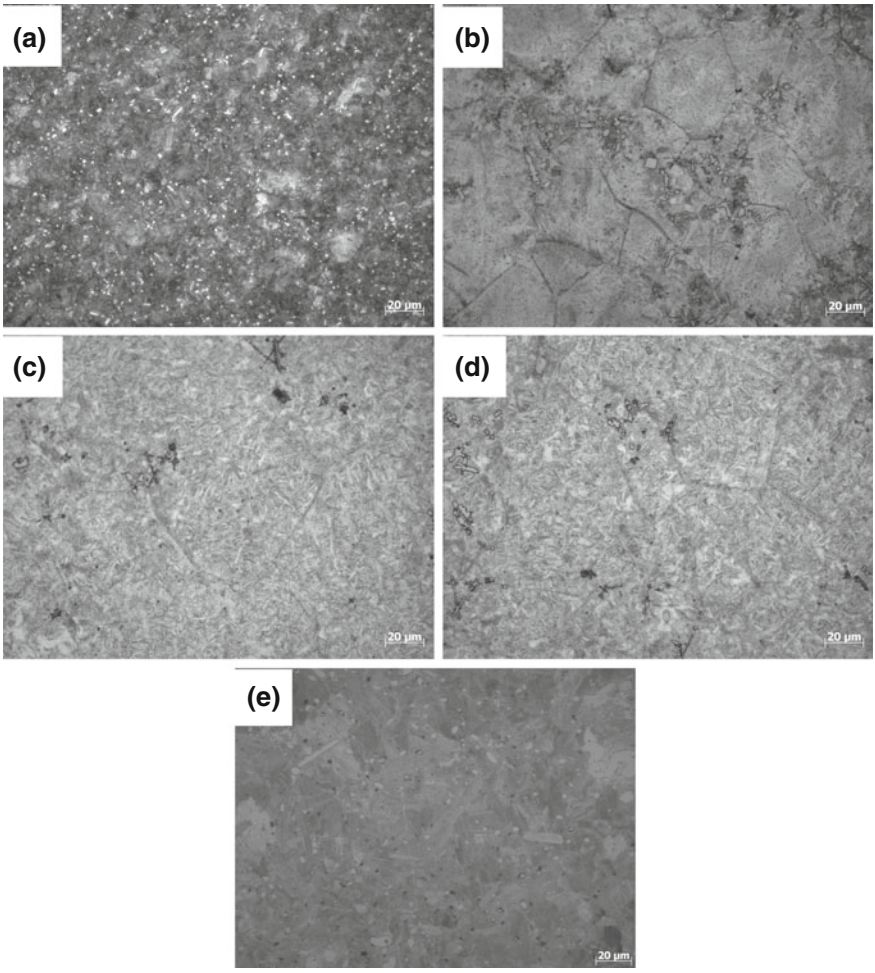

Fig. 2 Corrosive metallographic pictures of as-cast U–Zr alloy samples. **a** U–2 wt% Zr, **b** U–4 wt % Zr, **c** U–6 wt% Zr, **d** U–8 wt% Zr, **e** U–10 wt% Zr

organization increases. And the stability of the metastable organization in the alloy with high contents of Zr is improved.

X-ray tests are made on all alloys, as shown in Fig. 4. Most of components are α-U, and when the content of Zirconium reaches 10% there appeared α-U + δ phase.

Microstructure Analysis of the Alloy after the Homogenization Annealing. The sample of spray cast is treated with homogenization annealing. First, polish the sample. Then the microstructure of the sample is observed by the image analyzer.

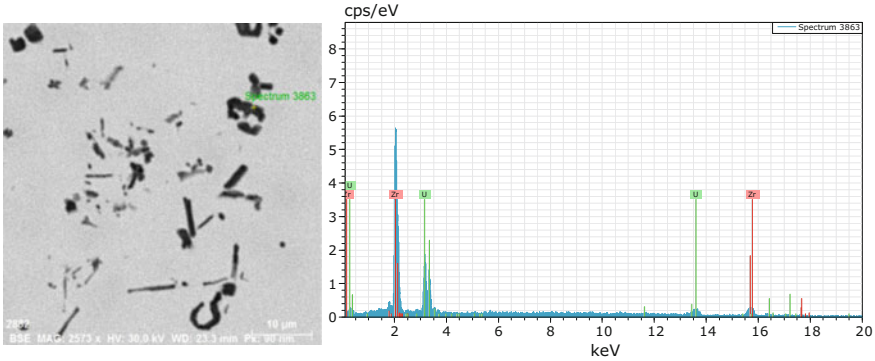

Element	Weigh percentage(%)	Atom percentage(%)
Zr	56.79	77.42
U	43.21	22.58

Fig. 3 Spectrum analysis of U–Zr alloy spray casting sample

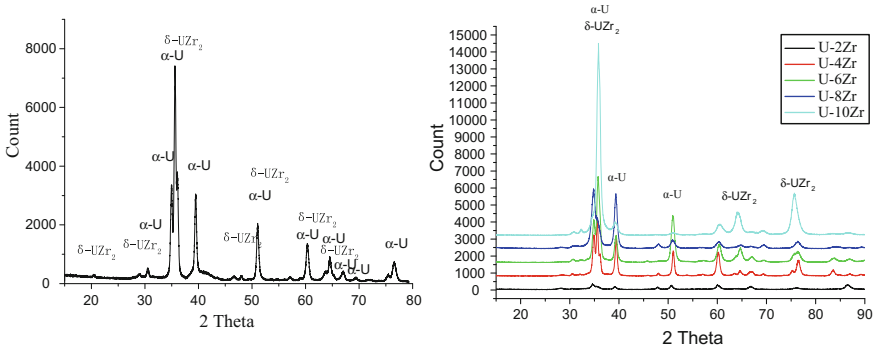

Fig. 4 XRD curve of as cast alloy samples

Fig. 5 Quenching metallographic picture of U–4 wt% Zr alloy sample

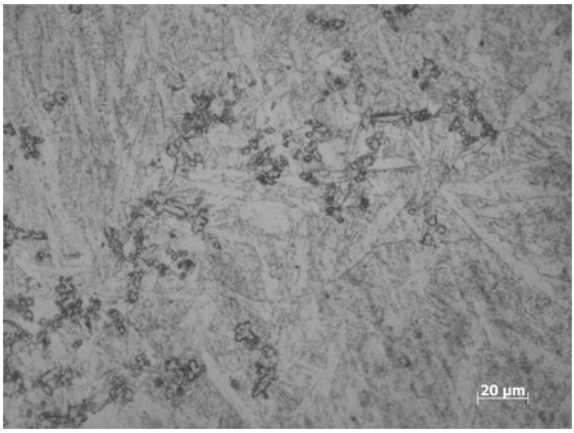

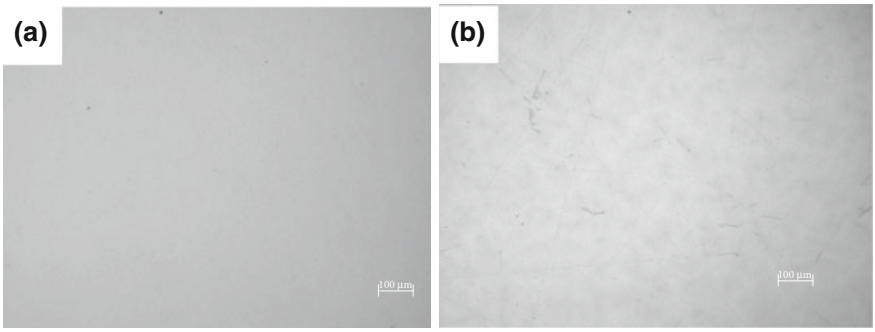

Fig. 6 Metallographic structure of U–Zr alloys after homogenization annealing. **a** U–2 wt% Zr, **b** U–10 wt% Zr)

Figure 6 is the pictures of polished U–2 wt% Zr and U–10 wt% Zr. The surface of the sample is smooth. And there are no obvious inclusion and incomplete fusions.

Figure 7 shows the metallographic picture after the Homogenization annealing of U–Zr alloy. Figure 7a, b show the U–2 wt% Zr, U–4 wt% Zr state respectively. The microstructure is layered, which is similar to the pearlite state of steel. And with the increase content of zirconium, layers of microstructure progressively refinement. Figure 7c is the metallographic photograph of U–6 wt% Zr alloy; the microstructure is shown as the lath-like interleaved distribution. With the content of Zr increased, the microstructure of U–8 wt% Zr alloy is similar to the twin structures in the pearlite (Fig. 7d). When the content of Zr is 10 wt%, the twin morphology of organization is more apparent and become finer (Fig. 7e).At the same time characteristic of pearlite is further weakened.

Homogenizing annealing is approximately equal to balance cooling. Figure 8 is equilibrium phase diagram of U–Zr alloy [2]. According to the phase diagram, the phase transformation of U–2–10 wt% of Zr alloy is from hypereutectoid to eutectoid transformation, and then the hypereutectoid transformation. The phase undergoes the transformation from a single γ phase to $\gamma' + \beta(U)$. As the temperature drops the phase become $\beta(U)$, $\alpha(U)$ and Zr-rich phase $\beta(Zr)$, finally it becomes $\alpha(U) + \delta$ phase at room temperature. With the content of Zr increases, it is difficult to undergo the solid diffusion transformation. And because of the pinning effect of Zr elements, microstructure transform in the form of twin change, Fig. 7e obviously shows the typical twin microstructure.

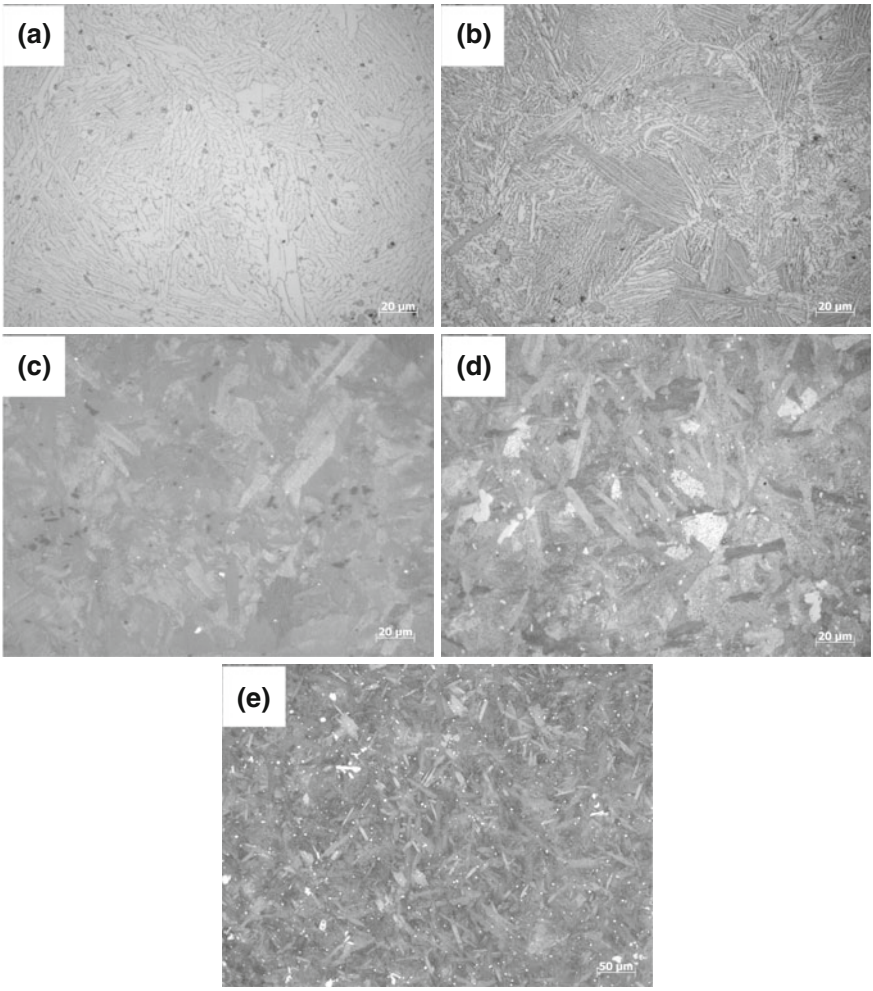

Fig. 7 Metallographic microstructure of U–Zr alloys after homogenization annealing. **a** U–2 wt% Zr, **b** U–4 wt% Zr, **c** U–6 wt% Zr, **d** U–8 wt% Zr, **e** U–10 wt% Zr

A spectral analysis of light objects is demonstrated in Fig. 9. The results show that it is U–75 wt% Zr. According to the phase diagram, during the cooling process of melting, the Zr-rich phase firstly precipitated, and then the structure of the near balance is formed. So the light colored parts of the alloy are considered to be Zr-rich phase and the grey matrix is the (α-U + δ) phase.

X-ray tests are made on all alloys, as shown in Fig. 10. Most of components are α-U, and when the content of Zirconium reaches 10% there appeared δ phase.

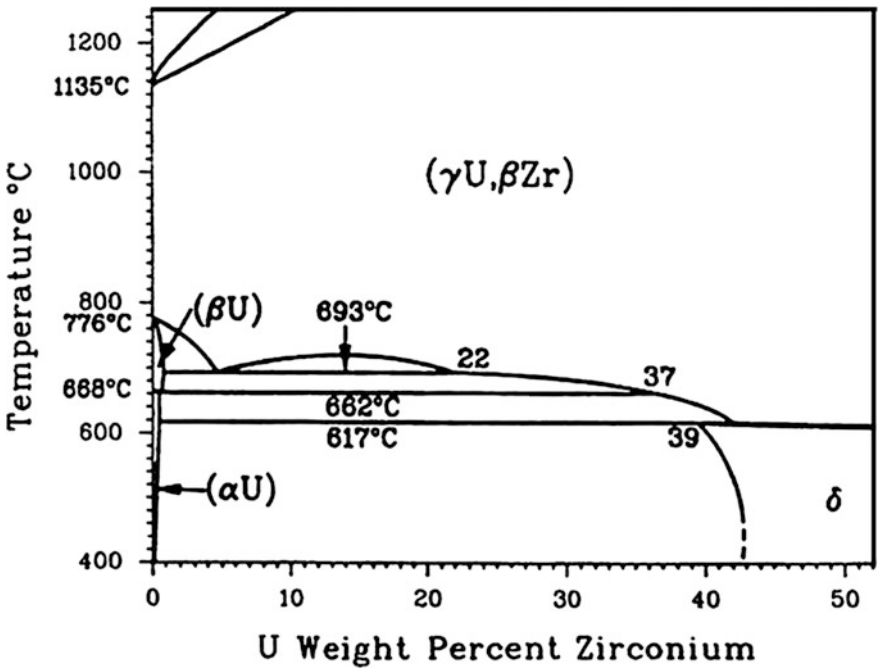

Fig. 8 Phase diagram of U–Zr alloy

Physical performance tests. The physical properties such as heat capacity (specific heat), thermal conductivity (heat conductivity) and thermal expansion coefficient are tested. A graph of data trends for different alloys is shown as follow.

As shown in the Fig. 11, with the increase of temperature the specific heat turn to slow down, and the lowest point is at 350 °C. Then it slowly rising, jump greatly at 700 °C. The whole process is relatively stable.

The thermal conductivity is obtained through multiplying the heat diffusion coefficient, density and the specific heat capacity, as shown in Fig. 12. From room temperature to 600 °C, the thermal diffusion coefficient increases as the temperature rises gradually. There has a little change when the temperature is a little higher than 600 °C. According to the phase diagram, at 612 °C $\alpha + \delta \rightarrow \alpha + \gamma 2$ transformation occurs, after that the phase transition also occurs at 659 °C and 688 °C. It is due to the fluctuation of thermal diffusion coefficient. When the temperature is higher than 720 °C it comes into single phase zone, and the thermal diffusion coefficient is rising fast.

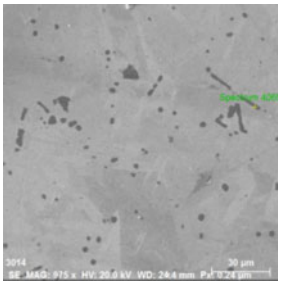

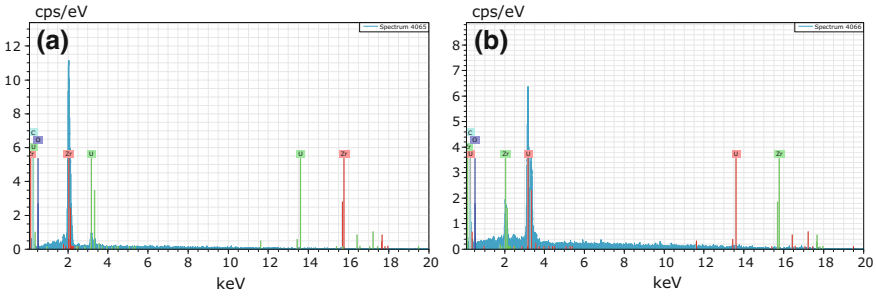

element	data of Fig.a		element	data of Fig.b	
	weigh percentage(%)	atom percentage(%)		weigh percentage(%)	atom percentage(%)
U	15.01	6.25	U	85.40	47.27
Zr	75.99	65.22	Zr	10.53	15.20

Fig. 9 Spectral analysis data of U–Zr alloy after annealing

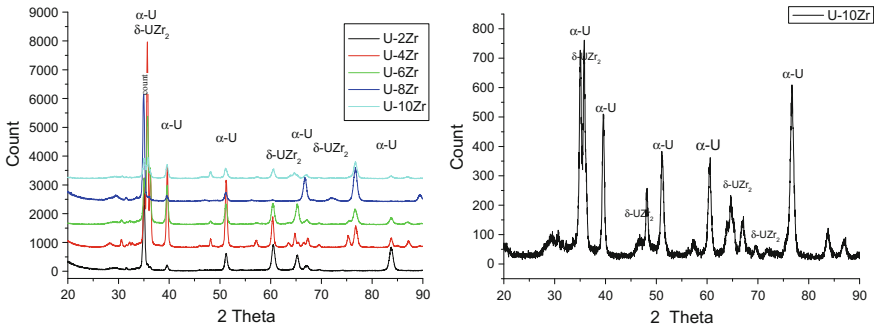

Fig. 10 XRD curve of U–Zr alloy after homogenization annealing

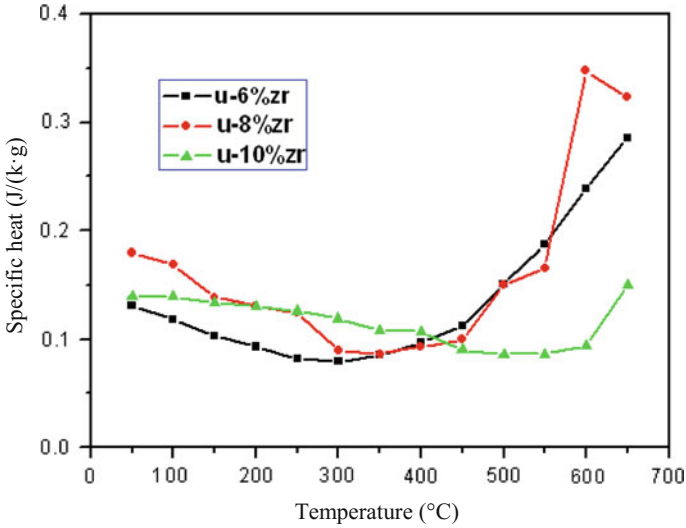

Fig. 11 Specific heat curves of U–Zr alloys

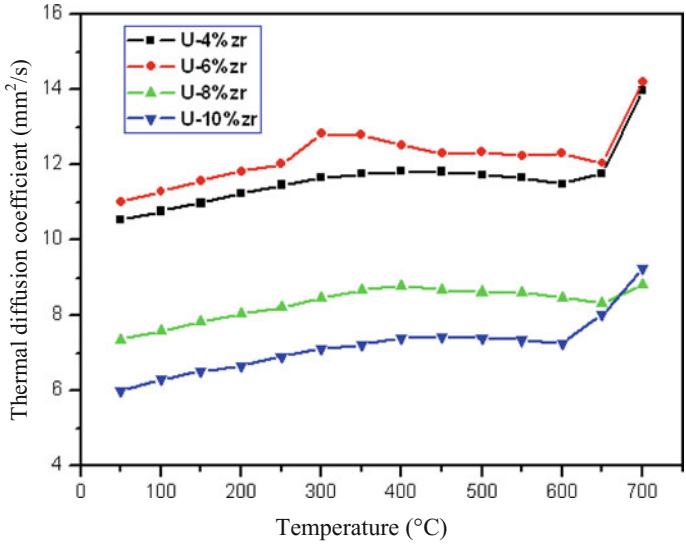

Fig. 12 Thermal diffusion coefficient of the U–Zr alloys

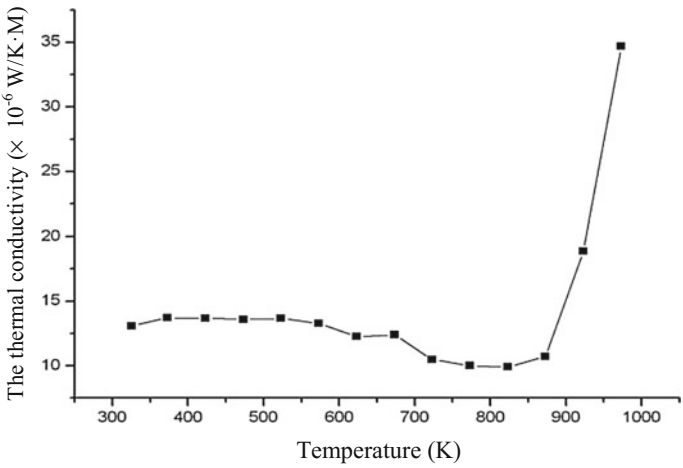

Fig. 13 Thermal conductivity-temperature curve of U–10 Zr

Based on heat diffusion coefficient, density and specific heat the thermal conductivity under different temperatures can be obtained (assuming that the density varies rarely with temperature). The thermal conductivity change process of U–10 Zr alloy is shown in Fig. 13. With the increase of temperature the alloy thermal conductivity firstly drops. After 900 K it rises rapidly.

As shown in Fig. 14, thermal expansion coefficient of U–10% Zr increases with the increase of temperature, at 700 °C it reaches the maximum: 18.57×10^{-6}/°C.

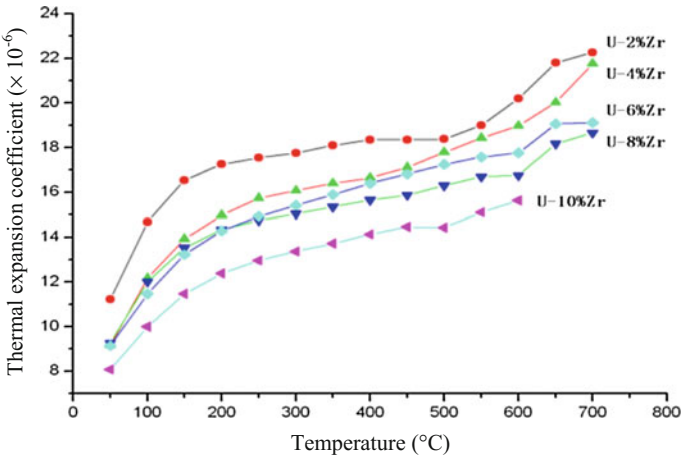

Fig. 14 Thermal expansion coefficient-temperature curve of U–Zr

Conclusions

When the cooling speed of U–Zr alloy is fast, as-cast microstructure morphology is characterized by liquid quenching microstructure, there is a clear grain boundary, at the same time the acicular structure characteristics is shown within the grain boundary. With the increase of Zr content, microstructure of acicular morphology is more apparent, but is relatively smaller. The microstructure of U–10 wt% Zr alloy is shown in the shape of the lath-like interleaved distribution, and in the interior of the lath-like microstructure two kinds of phase is interleaved by lamellar structure distribution. And the number and size of the rich-zirconium phase in the matrix are increasing gradually.

The microstructure of U–Zr alloy after homogenization annealing is layered, which is similar to the pearlite of steel. With the content of zirconium increases, the microstructure of layer is gradually refined. The microstructure of U–6 wt% Zr alloy is shown in the shape of the lath-like interleaved distribution. With the content of Zr increases, twin structures appear in the U–8 wt% Zr alloy which is similar to the pearlite. When the content of Zr is 10 wt%, the twin morphology of organization is more apparent and becomes finer. At the same time characteristic of pearlite is further weakened in the organization.

The specific heat slowly declines with the increase of temperature and reaches the lowest at 350 °C, and then slowly rises. From room temperature to 600 °C the thermal diffusion coefficient increases as the temperature rises gradually. Between 600 °C and 690 °C there are fluctuations. From 720 °C, thermal diffusion coefficient is rising fast.

References

1. L.C. Walters, Thirty years of fuels and materials information from EBR-II. J. Nucl. Mater. **270**, 39–48 (1999)
2. C.B. Basak, Microstructural evaluation of U-rich U–Zr alloys under near-equilibrium condition. J. Nucl. Mater. **416**, 280–287 (2011)